Title

Prospective emission efficiency and in-plane light polarization of nonpolar m-plane InxGa1-xN/GaN blue light emitting diodes fabricated on freestanding GaN substrates

Journal

Applied Physics Letters, 89(9)

ISSN

0003-6951

Authors

Koyama, T
Onuma, T
Masui, H
et al.

Publication Date

2006-08-01

Peer reviewed

Prospective emission efficiency and in-plane light polarization of nonpolar *m*-plane $In_xGa_{1-x}N/GaN$ blue light emitting diodes fabricated on freestanding GaN substrates

T. Koyama and T. Onuma
Institute of Applied Physics, University of Tsukuba, Tsukuba 305-8573, Japan and NICP, ERATO, Japan Science and Technology Agency, Kawaguchi 332-0012, Japan

H. Masui, A. Chakraborty, B. A. Haskell, S. Keller, U. K. Mishra, J. S. Speck, S. Nakamura, and S. P. DenBaars
Department of Materials Engineering, University of California, Santa Barbara, California 93106; Department of Electrical and Computer Engineering, University of California, Santa Barbara, California 93106; and NICP, ERATO, Japan Science and Technology Agency, Kawaguchi 332-0012, Japan

T. Sota
Department of Electrical Engineering and Bioscience, Waseda University, Shinjuku 169-8555, Japan

S. F. Chichibu[a)]
Institute of Applied Physics, University of Tsukuba, Tsukuba 305-8573, Japan and NICP, ERATO, Japan Science and Technology Agency, Kawaguchi 332-0012, Japan

(Received 15 May 2006; accepted 27 June 2006; published online 28 August 2006)

Prospective equivalent internal quantum efficiency (η_{int}) of approximately 34% at 300 K was demonstrated for the blue emission peak of nonpolar *m*-plane $(1\bar{1}00)$ $In_xGa_{1-x}N/GaN$ multiple quantum well light emitting diodes (LEDs) fabricated on freestanding *m*-plane GaN substrates. Although the η_{int} value is yet lower than that of conventional *c*-plane blue LEDs (>70%), the results encourage one to realize high performance green, amber, and red LEDs by reducing the concentration of nonradiative defects, according to the absence of the quantum-confined Stark effects due to the polarization fields parallel to the quantum well normal. The electric field component of the blue surface emission was polarized perpendicular to the *c* axis with the in-plane polarization ratio of 0.58 at 300 K. © *2006 American Institute of Physics*.
[DOI: 10.1063/1.2337085]

Wurtzite (Al, In, Ga)N materials provide enormous practical benefits in producing UV, blue, green, and white light emitting diodes (LEDs) and 405 nm laser diodes (LDs).[1] These devices employ *c*-plane $In_xGa_{1-x}N$ quantum wells (QWs) because the localized exciton emission[2] in InGaN exhibits high internal quantum efficiency (η_{int}) despite the presence of high density threading dislocations (TDs).[1] However, η_{int} decreases abruptly when the emission wavelength exceeds 500 nm (the InN molar fraction $x>0.2$)[3] due to the decrease in oscillator strength of electron-hole pairs, i.e., wave function separation due to the quantum-confined Stark effects (QCSEs). This is caused by the electrostatic fields (F_{pol}) parallel to the QW normal due to the spontaneous and piezoelectric polarizations.[2–5] Distinct from *polar* *c*-plane QWs, those grown in *nonpolar* orientations such as *a*-plane $(11\bar{2}0)$ and *m*-plane $(1\bar{1}00)$ do not suffer from QCSEs,[6–11] because the polar *c*-axis lies in the QW plane. Accordingly, high η_{int} can be expected for nonpolar LEDs[12,13] even when highly strained QWs are contained. In addition, nonpolar LEDs are expected to show in-plane optical anisotropy[6,14] according to the polarization selection rules. The polarized light[6,15] could be desirable for the backlighting of liquid crystal displays.

In this letter, steady-state, dynamical, and polarized optical responses of *m*-plane InGaN multiple quantum well (MQW) blue LED structures[13] are shown to demonstrate the prospective characteristics of nonpolar LEDs.

The LED structures[13] were grown by metal organic vapor phase epitaxy on *m*-plane free-standing GaN (FS-GaN) prepared by halide vapor phase epitaxy.[16] The densities of basal plane stacking fault and TD were determined from transmission electron microscope images (1×10^5 cm^{-1} and 4×10^9 cm^{-2}, respectively).[16] The active region was a five-period 4-nm-thick $In_{0.17}Ga_{0.83}N$/16-nm-thick GaN MQW. A photovoltaic (PV) spectrum at 300 K was taken using a monochromatic light source. Steady-state photoluminescence (PL) of the MQW was selectively excited with the 392.0 nm line of a cw InGaN LD (5 mW). Time-resolved photoluminescence (TRPL) was excited by a frequency-doubled (365 nm) mode-locked Al_2O_3:Ti laser (100 fs, 120 nJ/cm^2).

The PV spectrum of the LED exhibited a broad absorption tail (3.2~2.6 eV) and a superficial peak at 3.36 eV, as shown in Fig. 1. The decrease in the PV intensity for photon energies higher than 3.36 eV is due to the light absorption by the top *p*-type GaN. From the results that the PL spectrum exhibited multiple broad emission bands (dotted line) and the color of the electroluminescence (EL) differed from position to position over 10 μm length scales within a LED mesa (observed with a microscope), the local band gap variation is considered to originate from the variation of In-incorporation efficiency due to the presence of inclined planes and facets, as is the case with *a*-plane InGaN QWs.[11,13] Note that the color of the emission from each position did not change with LED current. However, spatially integrated EL spectra showed a superficial blueshift with increasing current, be-

[a)]Author to whom correspondence should be addressed; electronic mail: optoelec@bk.tsukuba.ac.jp

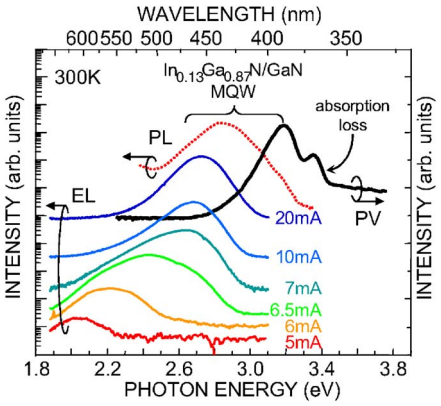

FIG. 1. (Color online) PV, PL, ad EL spectra of the *m*-plane InGaN/GaN MQW blue LED fabricated on the freestanding GaN substrate.

cause the current was progressively injected to the higher band gap regions: the emission colors were red (5 mA), yellow (6 mA), green (6.5 mA), and blue (>10 mA), as shown in Fig. 1. The results indicate the possibility to fabricate red to blue LEDs using proper orientations and growth conditions.

To verify the absence of F_{pol} parallel to the QW normal, selectively excited PL spectra of the LED were measured as a function of external bias (V_{EX}), as shown in Fig. 2. The intensity of the MQW emission around 2.75 eV decreased with the increase in magnitude of reverse bias (V_R) because of the tunneling escape of carriers from the QW. The intensity of the yellow luminescence band of the GaN substrate did not change with V_{EX}, as expected. An important finding is that the MQW emission did not show a remarkable peak shift with V_{EX}, implying the absence of strong F_{pol}. This result is different from the case for *c*-plane InGaN QWs, in which the QW emission exhibited a remarkable blueshift[17] with increasing V_R, because V_R weakened the piezoelectric F_{pol} within the InGaN QW.

Recombination dynamics of the MQW emission were examined on the unprocessed LED wafer, which had less In in the InGaN wells. PL spectrum of the wafer exhibited multiple PL peaks at 3.18, 2.95, and 2.79 eV at 8 K, which are labeled V, P, and B, respectively, as shown in Fig. 3(a) (details are discussed later). The TRPL signal for B peak is

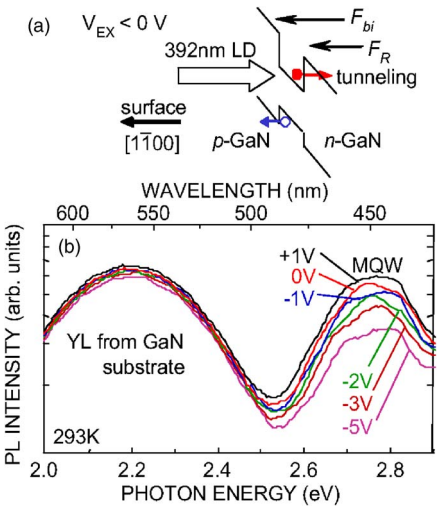

FIG. 2. (Color online) (a) Schematic band diagram of an *m*-plane InGaN QW under external bias V_{EX}. PL from the MQW was selectively excited with the 392.0 nm InGaN LD. (b) PL spectra of the LED under V_{EX}.

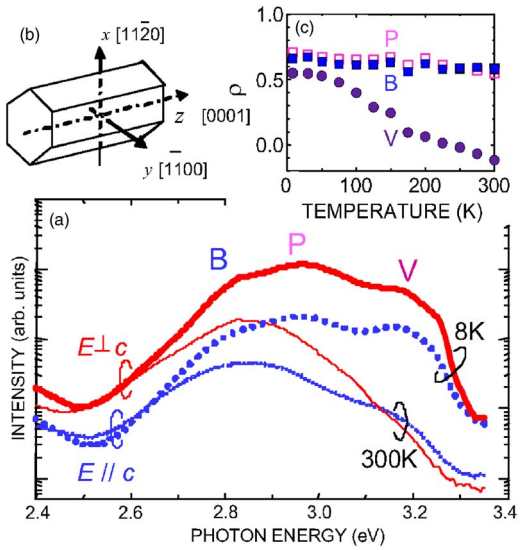

FIG. 3. (Color online) (a) Polarized PL spectra of the *m*-plane InGaN/GaN MQW LED wafer measured at 8 and 300 K; (b) definition of crystal axes; and (c) polarization ratios of V, P, and B peaks as a function of temperature.

shown as a function of temperature T in Fig. 4(a). The signal exhibited a nonidentical decay shape from 10 to 300 K, which can be fitted by a *stretched exponential* function. Peaks P and V showed similar results. These results indicate that localized exciton recombination dominates the MQW emission. Spectrally integrated B peak intensity is shown as a function of $1/T$ in Fig. 4(b). Values of η_{int} were 34% for B, 10% for P, and 2% for V peaks, respectively. We note that η_{int} was approximated as the integrated PL intensity at 300 K divided by that at 8 K. These values are comparable to those of *a*-plane InGaN MQWs grown on GaN templates prepared by lateral epitaxial overgrowth.[11] Because the TRPL signal exhibited a nonexponential decay shape, effective PL lifetime (τ_{eff}) was defined as the time after excitation when $\int_0^{\tau_{\mathrm{eff}}} I(t)dt / \int_0^{t_{\mathrm{lim}}} I(t)dt$ became $1-1/e$, where $I(t)$ is the intensity at time t and t_{lim} is the time when $I(t_{\mathrm{lim}})$ becomes $0.01I(0)$. The value of τ_{eff} for the B peak is plotted as a function of T by open triangles in Fig. 4(c). The effective

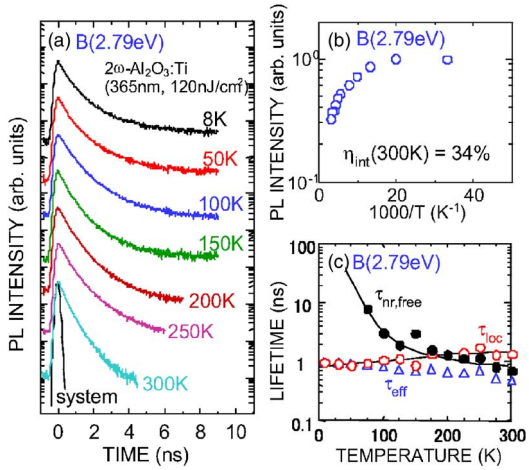

FIG. 4. (Color online) (a) TRPL signal and (b) integrated PL intensity of B peak (2.79 eV) in the *m*-plane InGaN MQW LED wafer measured at various T. (c) Effective PL lifetime τ_{eff} of B peak as a function of T (open triangles). Effective radiative lifetime of localized excitons (τ_{loc}) and effective nonradiative lifetime in the free and extended states ($\tau_{\mathrm{nr,free}}$) derived from τ_{eff} and η_{int} are also plotted by open and closed circles, respectively. The solid lines are drawn to guide the eyes.

radiative lifetime of localized excitons (τ_{loc}) and effective nonradiative lifetime in the free and extended states ($\tau_{nr,free}$) were calculated[18] using the relations $1/\tau_{eff}=1/\tau_{loc}+1/\tau_{nr,free}$ and $\eta_{int}=1/(1+\tau_{loc}/\tau_{nr,free})$, and are plotted in Fig. 4(c) by open and closed circles, respectively. The τ_{loc} value at 8 K ($\sim$1 ns) is shorter than that of *c*-plane QWs and is comparable to those of nonpolar *a*-plane[11] and cubic[18] InGaN QWs. The result again indicates the absence of F_{pol}. As shown, τ_{loc} is nearly independent of T ($\sim$1.4 ns at 300 K), indicating that excitons are localized and thermal escape to the two-dimensional space is suppressed. Because the present MQW has high density of nonradiative recombination centers, η_{int} is yet 34% at 300 K. Further reduction in both structural and point defect density is necessary to improve η_{int}.

Figure 3(a) shows the PL spectra of the LED wafer measured at 8 and 300 K under the light polarization E perpendicular to the *c*-axis ($E\perp c$) and E parallel to the *c*-axis ($E\| c$), where E is the electric field component. As shown, all V, P, and B peaks are predominantly polarized to $E\perp c$ at 8 K. Note again that these peaks are generated in different areas. The valence bands (VBs) of wurtzite GaN have symmetries Γ_{9v} [heavy hole (HH)], Γ_{7v}^{u} [light hole (LH)], and Γ_{7v}^{l} [crystal field split-off hole (CH)] in order of decreasing electron energy. Excitons associated with the respective VBs are referred to as A, B, and C excitons, respectively. Because VB is mainly constructed by *p*-like orbitals with wave functions of $|X\pm iY\rangle$ for the HH and LH bands and of $|Z\rangle$ for the CH band, A and B transitions are allowed for $E\perp c$ and C transition is allowed for $E\| c$. In the case of *m*-plane InGaN on GaN, the in-plane [*x*-*z* plane; see Fig. 3(b)] anisotropic compressive strain breaks the symmetry in the *x*-*y* plane of the wurtzite crystal, resulting in the change of crystal symmetry from C_{6v} to C_{2v}. Under such circumstances, original $|X\pm iY\rangle$ VB states are broken into $|X\rangle$-like and $|Y\rangle$-like ones.[19–21] Accordingly, VBs are reconstituted to $|X\rangle$-like, $|Z\rangle$-like, and $|Y\rangle$-like ones in order of decreasing electron energy. Therefore, the transition lowest in energy is allowed for $E\perp c$, and the transition involving the $|Z\rangle$-like VB must occur at the higher energy under $E\| c$. Although the emissions from the MQW were polarized to $E\perp c$, observable peak shift could not be found, as shown in Fig. 3(a), because the spectral broadening was too large. The polarization ratios (ρ) of the respective peaks are plotted as a function of T in Fig. 3(c). The value of ρ was defined as $(I_{\perp}-I_{\|})/(I_{\perp}+I_{\|})$, where $I_{\perp}$ and $I_{\|}$ are PL intensities for $E\perp c$ and $E\| c$, respectively. Because the thermal distribution of carriers in the second lowest $|Z\rangle$-like VB is negligible at low T, ρ values close to unity are expected at 8 K. However, ρ values were as small as 0.55, 0.71, and 0.66 for V, P, and B peaks, respectively. Possible causes are (i) mixing of the $|X\rangle$-like and $|Z\rangle$-like VB states and (ii) zero-dimensional nature of the localizing radiative centers. The ρ values of P and B peaks were nearly independent of T: they were 0.55 for P and 0.58 for B at 300 K. This result can be explained by the large VB splitting[6] between the $|X\rangle$ and $|Z\rangle$ states due to the large compressive strain in the InGaN wells, which results in negligible carrier distribution in the $|Z\rangle$ state even at elevated T. The decrease in the ρ value in response to a temperature rise for the V peak may be due to small VB splitting of the $In_xGa_{1-x}N$ wells of low x.

In summary, we showed prospective emission characteristics of nonpolar *m*-plane InGaN MQW LEDs. Although the LED had macroscopic in-plane band gap variation due to the presence of inclined planes and facets, η_{int} value of 34% at 300 K was demonstrated for the blue emission peak, according to the beneficial effects of localized excitons. The absence of the polarization fields parallel to the QW normal was confirmed by TRPL and selective excitation PL measurements. Since the blue MQW emission is polarized to $E\perp c$ with the polarization ratio of 0.58, *m*-plane InGaN LEDs have a potential for the use in high η_{int}, polarization-sensitive optoelectronic devices.

This work was supported in part by the 21st Century COE program.

[1]For example, see S. Nakamura and G. Fasol, *The Blue Laser Diode* (Springer, Berlin, 1997); see also I. Akasaki and H. Amano, Jpn. J. Appl. Phys., Part 1 **36**, 5393 (1997).
[2]S. Chichibu, T. Azuhata, T. Sota, and S. Nakamura, Appl. Phys. Lett. **69**, 4188 (1996); S. F. Chichibu, A. C. Abare, M. P. Mack, M. S. Minsky, T. Deguchi, D. Cohen, P. Kozodoy, S. B. Fleischer, S. Keller, J. S. Speck, J. E. Bowers, E. Hu, U. K. Mishra, L. A. Coldren, S. P. DenBaars, K. Wada, T. Sota, and S. Nakamura, Mater. Sci. Eng., B **59**, 298 (1999).
[3]S. F. Chichibu, T. Sota, K. Wada, O. Brandt, K. H. Ploog, S. P. DenBaars, and S. Nakamura, Phys. Status Solidi A **183**, 91 (2001).
[4]T. Takeuchi, S. Sota, M. Katsuragawa, M. Komori, H. Takeuchi, H. Amano, and I. Akasaki, Jpn. J. Appl. Phys., Part 2 **36**, L382 (1997).
[5]F. Bernardini and V. Fiorentini, Phys. Rev. B **57**, R9427 (1998).
[6]P. Waltereit, O. Brandt, A. Trampert, H. T. Grahn, J. Menniger, M. Ramsteiner, M. Reiche, and K. H. Ploog, Nature (London) **406**, 865 (2000); Y. J. Sun, O. Brandt, M. Ramsteiner, H. T. Grahn, and K. H. Ploog, Appl. Phys. Lett. **82**, 3850 (2003).
[7]H. M. Ng, Appl. Phys. Lett. **80**, 4369 (2002).
[8]E. Kuokstis, C. Q. Chen, M. E. Gaevski, W. H. Sun, J. W. Yang, G. Simin, M. A. Khan, H. P. Maruska, D. W. Hill, M. C. Chou, J. J. Gallagher, and B. Chai, Appl. Phys. Lett. **81**, 4130 (2002).
[9]M. D. Craven, P. Waltereit, F. Wu, J. S. Speck, and S. P. DenBaars, Jpn. J. Appl. Phys., Part 2 **42**, L235 (2003); Appl. Phys. Lett. **84**, 496 (2004).
[10]T. Koida, S. F. Chichibu, T. Sota, M. D. Craven, B. A. Haskell, J. S. Speck, S. P. DenBaars, and S. Nakamura, Appl. Phys. Lett. **84**, 3768 (2004).
[11]T. Onuma, A. Chakraborty, B. A. Haskell, S. Keller, S. P. DenBaars, J. S. Speck, S. Nakamura, U. K. Mishra, T. Sota, and S. F. Chichibu, Appl. Phys. Lett. **86**, 151918 (2005).
[12]C. Q. Chen, V. Adivarahan, J. W. Yang, M. Shatalov, E. Kuokstis, and M. A. Khan, Jpn. J. Appl. Phys., Part 2 **42**, L1039 (2003).
[13]A. Chakraborty, B. A. Haskell, S. Keller, J. S. Speck, S. P. DenBaars, S. Nakamura, and U. K. Mishra, Appl. Phys. Lett. **85**, 5143 (2004); Jpn. J. Appl. Phys., Part 2 **44**, L173 (2005).
[14]K. Domen, K. Horino, A. Kuramata, and T. Tanahashi, Appl. Phys. Lett. **71**, 1996 (1997).
[15]H. Masui, A. Chakraborty, B. A. Haskell, U. K. Mishra, J. S. Speck, S. Nakamura, and S. P. DenBaars, Jpn. J. Appl. Phys., Part 2 **44**, L1329 (2005).
[16]B. A. Haskell, A. Chakraborty, F. Wu, H. Sasano, P. T. Fini, S. P. DenBaars, J. S. Speck, and S. Nakamura, J. Electron. Mater. **34**, 357 (2005).
[17]T. Takeuchi, C. Wetzel, S. Yamaguchi, H. Sakai, H. Amano, I. Akasaki, Y. Kaneko, S. Nakagawa, Y. Yamaoka, and N. Yamada, Appl. Phys. Lett. **73**, 1691 (1998); S. F. Chichibu, T. Azuhata, T. Sota, T. Mukai, and S. Nakamura, J. Appl. Phys. **81**, 5153 (2000).
[18]Definitions of τ_{eff}, τ_{loc}, and $\tau_{nr,free}$ are given in S. F. Chichibu, T. Onuma, T. Aoyama, K. Nakajima, P. Ahmet, T. Chikyow, T. Sota, S. P. DenBaars, S. Nakamura, T. Kitamura, Y. Ishida, and H. Okumura, J. Vac. Sci. Technol. B **21**, 1856 (2003).
[19]A. Alemu, B. Gil, M. Julier, and S. Nakamura, Phys. Rev. B **57**, 3761 (1998).
[20]S. Ghosh, P. Waltereit, O. Brandt, H. T. Grahn, and K. H. Ploog, Phys. Rev. B **65**, 075202 (2002).
[21]P. Paskov, T. Paskova, P. O. Holtz, and B. Monemar, Phys. Status Solidi A **190**, 75 (2002).